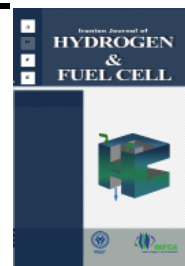


Iranian Journal of Hydrogen & Fuel Cell

IJHFC

Journal homepage://ijhfc.irost.ir



Modeling and simulation of a new architecture stack applied on the PEM fuel cell

A.Torkavannejad*, N. Pourmahmoud

Department of Mechanical Engineering, Urmia University, Urmia, Iran

Article Information

Article History:

Received:

27 July 2016

Received in revised form:

07 Oct 2016

Accepted:

29 Oct 2016

Keywords

Fuel cell
PEM fuel cells
Single-phase
Geometry

Abstract

To simulate a new economical architecture for PEM fuel cells and investigate the effectiveness of the introduced structure on the performance, computational fluid dynamics (CFD) code is used to solve the equations for a single domain of the cell namely: flow field, mass conservation, energy conservation, species transport, and electric/ionic fields under the assumptions of steady state and single phase. In this article, a new architecture of a proton exchange membrane fuel cell (PEMFCs) stack with typical geometry is presented in which every anode channel is in connection with two cathode channels over the constant length and vice versa. The analyzed numerical results yield to observation the effect of this new structure on distributions like current density oxygen, water, hydrogen mass fraction, current density and temperature. The introduced configuration has the same active area as the base model. The polarization curve for this new cell demonstrates that a straight channel with dual connections in each channel shows considerably better performance and greatly surpassed the current density region of the polarization curves of a fuel cell using the base structure. The improved model brings several advantages to the conventional PEMFC configuration: sufficient distribution of reactants in the flow field improvement in the concentration distribution along the channels and transport of the reactant gases through the gas diffusion layer (GDL), easy removal of produced water due to a shorter channel, and a lower cost of the PEMFC due to minimizing the total volume of the fuel cell. With regard to the polarization curve, application of this design is strongly recommended to obtain high current density in the operating condition and should be considered in the manufacture of a new generation of PEMFCs for high performance stacks.

*Corresponding Author's Fax: +98443337767

E-mail address: a.torkavannejad@urmia.ac.ir, Ph.D Candidate

1. INTRODUCTION

A PEM fuel cell is the most efficient simple mechanism device in which electrical energy with nearly zero emission can be attained by releasing the energy of a chemical reaction. Another prominent characteristic of this device is that more electricity can be generated for constant value fuel than other conventional energy conversion devices. Recently, a large number of studies and investigations have been conducted on the cost of manufacturing along with better performance and durability which are the main problems in the promotion of fuel cell technology. Many researchers are interested in achieving this goal in this area [1-4].

While researchers have tried to overcome these challenges [5-8], some issues remain unresolved [9, 10]. There are many important parameters that have a major effect on fuel cell performance such as: the system operating conditions, the chemical and mechanical properties of the components of the fuel cell and which is most applicable, and improvement of the gases distribution over the MEA by means of the gas channels geometry. The structure efficiency along with guiding and supplying reactants appropriately to obtain uniform current density inside the cell play crucial roles in PEMFC's performance, durability and cost [11,12]. More research must be done on the conventional PEMFC models in terms of technical, mechanical and economic problems. These problems include the high mass of the brittle graphite bipolar plates yielding a high value of weight and large occupied volume, the uneven distribution and low diffusion of reactants into the catalyst layer, working outside the standard range of temperature, and the low amount of outlet current density and performance. Some efforts have been made by researchers in order to ameliorate the performance using different configurations of the flow fields, such as inter-digitated, single serpentine and double serpentine, but investigations to present a better flow field are continually ongoing [13, 14]. Yu and Su [15] explored the two conventional serpentine and parallel configurations. Their obtained results show that a

serpentine flow channel demonstrates better operation over the parallel structure. Lorenzini-Gutierrez et al. [16] worked on a novel tree-shaped channel in radial form in order to overcome the pressure drop along with a larger reaction area which leads to higher values of current density. They concluded that their novel pattern is the best candidate among other proposed configurations due to cover all of the chemical reaction area and a low pressure drop along the channel. Sierra et al. [17] introduced a concept combining the two conventional structures with a tubular structure and evaluated their combination's performance. Their obtained result showed that the conventional tubular form of fuel cell reduces the pressure losses to some extent and due to the easy eviction of produced water from the gas diffusion layer increases the species concentration in the reaction area. In their recent work, Pourmahmoud et al. [18] applied some revisions to the conventional configuration. They deflected the MEA in order to enlarge the reaction area in both anode and cathode side. Their introduced concept increased velocity in some parts of the flow channel and consequently increased the reactant transport causing cathode overpotential decrement, which is the main factor in preventing performance increment.

Nowadays researchers are focusing on the geometry of fuel cells. Their analysis have demonstrated that applying novel appropriate design has the greatest impact among other parameters. Models introduced have provided some benefits in certain aspects, but are still lacking in comparison with conventional designs. Some researchers have investigated spiral geometries but this structure has some drawbacks like difficulty in manufacturing. In this regard, Escobar et al. [19] simulated a spiral modification that revealed an even current density distribution and a smaller value of pressure losses. Juarez et al. [20] evaluated the advantages of a concentric spiral shape on the overall performance of a fuel cell stack using overpotential and power plots

drawn to investigate each structure. Radial flow has recently been presented by Cano et al. [21, 22]. They explored the effect of radial flow on velocity and the number of inlet flow fields on the outlet power. Their numerical results demonstrated that poor performance might be due to the low velocity value at the outlet region of the channels. As mentioned before, one parameters having a substantial effect on performance and has a direct association with performance is the reactants channel structure embed in the stack. Torkavannejad et al. [23] increased the outlet current density and reduced the cost and weight in order to increase the channel utilization, the main obstacle preventing the common and global usage of this simple technology. Furthermore, they changed the MEA arrangement so that every MEA is in connection with two cathodes and vice versa. With this arrangement, not only is the outlet performance increased remarkably, the bipolar, which is main and heaviest part, decreased about 40%. Wang et al. [24] improved a modification by embedding a baffle in a serpentine configuration allowing high performance to be achieved in PEMFCs at high current density. Additionally, in their study some dimension optimization, such as channel height, yielded better reactant transport to reaction area. Alvarado et al. [25] introduced a symmetric flow pattern which obtained higher performance due to a more efficient channel structure in spreading the reactants. Chen et al. [26] were involved with novel flow field modifications such as z-type and interdigitated channels. Recently some studies have been focused on enlarging and developing the reaction area to obtain a higher rate of chemical reaction along the channel [27-31]. Tiss et al. [32] studied partially blocked channel numerically and experimentally and its effect on performance and reactant transport. They also investigated the optimized angle of inclination. Their results showed that increasing the degree tilt up to 4.9 led to better performance but increasing this value more had the opposite effect. Walckzy et al. [33] provided uniform current density and a more economical cell by using ribbon MEA architectures. In another effort, Tseng et al. [34] proposed to use

metal foam as a flow distributor in order to reduce the weight and volume of the PEM fuel cell. Their investigation showed that the PEM fuel cell with this novel characteristic as a flow distributor presented some unique results compared with a conventional PEM unit cell with a traditional flow field plate as the flow distributor. Less mass transport limitation and lightweight plus better electrical conductivity are the main advantages of the introduced distributor plates. Bilgili et al. [35] performed simulations with an obstacle in their flow field at different boundary and inlet conditions. They concluded that by adding an obstacle in channel flow field, reactants diffusion and distribution can be improved through the gas diffusion layer (GDL) a significant amount which leads to performance improvement. Vazifeshenas et al. [36] introduced and investigated the effect of appropriate compound flow on the performance and water flooding. Their numerical simulation shows that there is a direct link between performance and channel design and flooding can be prevented by using a well-designed pattern. In this regard, their research showed that the compound design works as well as serpentine and in some cases remarkably better.

Khazaae et al. [37] recently proposed a novel first-of-its-kind architecture. They presented a unique annular and duct-shaped model for PEMFCs that solves some of the technical issues and greatly enhances the performance. This architecture may be the beginning of a new generation of fuel cells. According to the above explanation, designing an more appropriate structure provides a range of technical and economic benefits and this will only be achieved by moving from the conventional fuel cell to a new version of the structure. In this regard, a new version of the structure and MEA arrangement in line with our previous work has been simulated. Fig. 1 proposes a wave-liked MEA and flow field with a special arrangement of reactant supply channels that have the same mechanical, chemical and thermal properties as the base model. This type of PEMFC configuration has been introduced in order to enhance power generation, reduce the cost and weight of the stack, allow easier manufacturing,

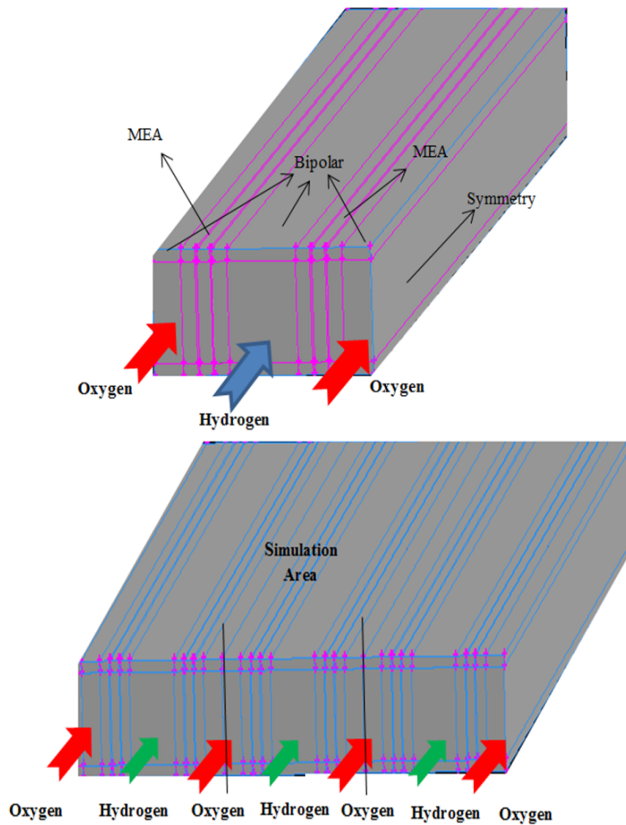


Fig. 1. Novel Architecture apply for PEMFC.

decrease species losses, improve the reactants distribution, and due to a shorter channel length easier eviction of water molecules which leads to an increases in channel efficiency. In the present study, we report the merit and operational consideration of employing the novel architecture over conventional PEMFCs in terms of chemical phenomenon, such as species, temperature and current distribution, inside the cell in order to clarify the effect of the novel flow pattern on the overall performance.

2. Model description

2.1 System description

Constant mass flow rate at the channel, inlet constant pressure condition at the channel outlet, and no-flux conditions are applied to the mass, momentum, species and potential conservation equations at all boundaries except for the inlets and outlets of the

anode and cathode flow channels. The side's faces are symmetrical.

Fig. 2 represents the conventional domain of the base model and Table 1 summaries the geometric parameters and operation conditions of the base model. The cell consists of hydrogen and oxygen channels, bipolar plates that act as a current collector with high electronic conductivity on the cathode and anode sides of the cell and the membrane electrode assembly (MEA) located between the gas channels.

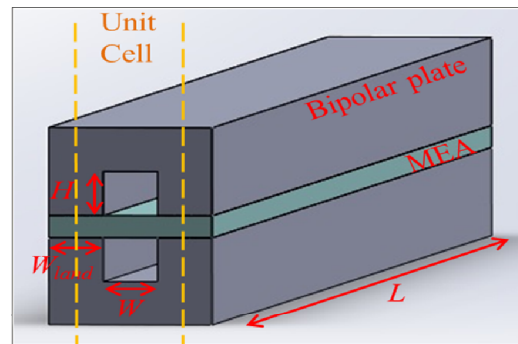


Fig. 2. Computational domain of base model.

Fig. 1 shows the configuration of the proposed fuel cell. This fuel cell has the same active and operation conditions as the base model. This allows for the comparison of PEMFC configurations in the same conditions. The reactant gases are supplied by inlet channels and leave the areas at the outer edge of the cell. As it is obvious in the figure, every cathode flow field is in contact with two anode reaction areas and vice versa. This configuration leads to the introduction of novel stacks, especially in terms of the way the reactants are supplied, less volume occupied due to having shorter lengths, and the potential for enhancing PEMFC performance. All geometric parameters of the novel architecture are presented in Table 2.

2.2 Model assumption

The model aims to study the electrochemical kinetics, current distribution, reactant flow fields and multi-component transport of oxidizer and fuel streams in a multi-dimensional domain. The model was built considering the following assumptions:

Table 1. Geometric parameters and operation conditions for base model

Parameter	Symbol	Value	Unit
Channel length	L	0.05	m
Channel width	W	1e_3	m
Channel height	H	1e_3	m
Land area width	Wland	1e_3	m
Gas diffusion layer thickness	dGDL	0.26e_3	m
Wet membrane thickness (Nafion 117)	δ_{mem}	0.23e_3	m
Catalyst layer thickness	δ_{CL}	0.0287e_3	m
Anode pressure	P _a	3	atm
Cathode pressure	P _c	3	atm
Inlet fuel and air temperature	T _{cell}	353.15	K
Relative humidity of inlet fuel and air (fully humidified conditions)	ψ	100	%
Reference current density	I	10	A/cm ²
Inlet anode oxygen mass fraction	Y _{OXYGEN,A}	0	-
Inlet anode hydrogen mass fraction	Y _{HYDROGEN,A}	0.3780066	-
Inlet anode water mass fraction	Y _{WATER,A}	0.6219934	-
Inlet cathode water mass fraction	Y _{WATER,C}	0.1031307	-
Inlet cathode oxygen mass fraction	Y _{OXYGEN,C}	0.2088548	-
Inlet cathode hydrogen mass fraction	Y _{HYDROGEN,C}	0	-
Membrane equivalent weight	-	1.1	Kg/mol

Table 2. Geometric parameters for simplified model (single cell)

	Base model	Flat shape
CHANNEL WIDTH (mm)	1	1.6
SHOULDER WIDTH(mm)	0.5	0.4
CELL LENGTH(mm)	50	25
GAS DIFFUSION THICKNESS(mm)	0.26	0.26
CATALYST LAYER THICKNESS(mm)	0.0287	0.0287
MEMBRANE THICKNESS(mm)	0.26	0.26

A non-isothermal steady state condition under constant load conditions .

All gases are assumed to obey ideal gas behaviors.

The gas diffusion layer and catalyst layers are homogeneous and isotropic porous mediums.

Flow is incompressible and laminar due to low pressure gradients and velocities.

The volume of liquid-phase water produced in the electrochemical reactions is negligible and phase change or two phase-transport is not considered, so this model is considered as a single phase. This issue may be reconsidered and added to the model in future work.

The membrane is impermeable to cross-over of reactant gases and assumed to be fully humidified.

The species diffusion and electrochemical reaction is

based on the dilute solution theory and Butler-Volmer kinetic equation, respectively.

A fully humidified inlet condition for the anode and cathode is used.

3. Model equations

3.1. Gas flow fields

In the fuel cell, the gas-flow field is obtained by solving the steady-state Navier-Stokes equations, i.e. the continuity equation:

$$\nabla \cdot (\rho u) = 0 \quad (1)$$

and momentum equations;

$$\nabla \cdot (\rho u \otimes u - \mu \nabla u) = -\nabla \left(P + \frac{2}{3} \mu \nabla u \right) + \nabla \cdot [\mu (\nabla u)^T] \quad (2)$$

The mass balance is described by the divergence of the mass flux through diffusion and convection. The steady state mass transport equation can also be written in the following expression for species:

$$\nabla \cdot [-\rho y_i \sum_{j=1}^N D_{ij} \frac{M}{M_j} \left(\nabla y_i + y_i \frac{\nabla M}{M} \right) + \rho y_i u] = 0 \quad (3)$$

where the subscript i denotes oxygen at the cathode side, and hydrogen at the anode side, and j is water vapor in both cases. Nitrogen is the third species at the cathode side.

The Maxwell-Stefan diffusion coefficients of any two species are dependent on temperature and pressure. They can be calculated according to the empirical relation based on the kinetic gas theory [19];

$$D_{ij} = \frac{T^{1.75} \times 10^{-3}}{P \left[\sum_k V_{ki} \right]^{\frac{1}{3}} + \left(\sum_k V_{kj} \right)^{\frac{1}{3}}]^2} \left[\frac{1}{M_i} + \frac{1}{M_j} \right]^{1/2} \quad (4)$$

In this equation, pressure is in [bar], and the binary diffusion coefficient is in [cm²/s]. The values for $\sum V_{ki}$ are given by Fuller et al., and the temperature field is obtained by solving the convective energy equation;

$$\nabla \cdot (\rho C_p u T - k \nabla T) = 0 \quad (5)$$

3.2. Gas diffusion layers

Transport in the gas diffusion layer is modeled as transport in a porous media. The continuity equation in the gas diffusion layers becomes:

$$\nabla \cdot (\rho \varepsilon u) = 0 \quad (6)$$

The momentum equation reduces to Darcy's law:

$$u = \frac{K_p}{\mu} \nabla P \quad (7)$$

The mass transport equation in porous media is:

$$\nabla \cdot [-\rho \varepsilon y_i \sum_{j=1}^N D_{ij} \frac{M}{M_j} \left(\nabla y_i + y_i \frac{\nabla M}{M} \right) + \rho \varepsilon y_i u] = 0 \quad (8)$$

In order to account for geometric constraints of the porous media, the diffusivities are corrected using the Bruggemann correction formula:

$$D_{ij}^{eff} = D_{ij} \times \varepsilon^{1.5} \quad (9)$$

The heat transfer in the gas diffusion layers is governed by:

$$\nabla \cdot (\rho \varepsilon C_p u T - k_{eff} \varepsilon \nabla T) = \varepsilon \beta (T_{solid} - T) \quad (10)$$

where, the term on the right-hand side accounts for where, the term on the right-hand side accounts for the heat exchange to and from the solid matrix of the GDL. Here, β is a modified heat transfer coefficient that accounts for the convective heat transfer in [W/m²] and the specific surface area [m²/m³] of the porous medium. Hence, the unit of β is [W/m³]. The potential distribution in the gas diffusion layers is:

$$\nabla \cdot (\lambda_c \nabla \phi) = 0 \quad (11)$$

3.3. Catalyst layers

The catalyst layer is treated as a thin interface, where sink and source terms for the reactants are implemented. Due to the infinitesimal thickness, the source terms are actually implemented in the last grid cell of the porous medium. At the cathode side, the sink term for oxygen can be written as:

$$S_{O_2} = -\frac{M_{O_2}}{4F} i_c \quad (12)$$

Whereas, the sink term for hydrogen is specified as:

$$S_{H_2} = -\frac{M_{H_2}}{4F} i_a \quad (13)$$

The production of water is modeled as a source term and hence can be given as:

$$S_{H_2O} = \frac{M_{H_2O}}{4F} i_c \quad (14)$$

The generation of heat in the cell is due to entropy changes as well as irreversibility due to the activation overpotential:

$$q = \left[\frac{T(-\Delta s)}{n_e F} + \eta_{act,c} \right] i_c \quad (15)$$

The local current density distribution in the catalyst layers can be modeled by the Butler-Volmer equation:

$$i_c = i_{O_2,C}^{ref} (C_{O_2} / (C_{O_2}^{ref})) \left[\exp((\alpha_a F) / RT) \eta_{act,c} + \exp((\alpha_c F) / RT) \eta_{act,c} \right] \quad (16)$$

$$i_a = i_{O_2,a}^{ref} (C_{H_2} / (C_{H_2}^{ref})) \left[\exp((\alpha_a F) / RT) \eta_{act,a} + \exp((\alpha_c F) / RT) \eta_{act,a} \right] \quad (17)$$

3.4. Membrane

The balance between the electro-osmotic drag of water from anode to cathode and back diffusion from cathode to anode yields the net water flux through the membrane:

$$N_w = n_d M_{H_2O} \frac{i}{F} - \nabla \cdot (\rho D_w \nabla y_w) \quad (18)$$

For heat transfer purposes, the membrane is considered a conducting solid, which means that the transfer of energy associated with the net water flux through the membrane is neglected. Heat transfer in the membrane is governed by:

$$\nabla \cdot (k_{mem} \nabla T) = 0 \quad (19)$$

The potential loss in the membrane is due to resistance of proton transport across the membrane which is equal to:

$$\nabla \cdot (\lambda_m \nabla \phi) = 0 \quad (20)$$

3.4. Boundary conditions

For the momentum conservation equation, fuel velocity is specified at each inlet of the anode and cathode flow channel. The velocity is calculated based on the concept of stoichiometry, which means "the required amount of fuel at a given condition". Boundary conditions are set as follows: constant mass flow rate at the channel inlet and constant pressure condition at the channel outlet, which means it discharges to the atmosphere. The inlet mass

fractions are determined by the inlet pressure and humidity according to the ideal gas law. Gradients at the channel exits are set to zero. The equations for both inlets are expressed as:

$$|\bar{u}|_{in} = \frac{\zeta}{X_{H_2,in}} \frac{I_{avg}}{2F} \frac{RT_{in}}{P_{in}} \frac{A_{MEA}}{A_{ch}}$$

Iavg is the average current density at a given cell-potential. Where, R, Tin, Pin, and ζ are the universal gas constant, temperature in the inlet, pressure in the inlet, and stoichiometric ratio, respectively. The stoichiometric ratio is defined as the ratio between the amount of supplied and the amount of required reactant on the basis of the reference current density Iavg, accordingly. The model parameter values are given in Table 1 and 2, and the inlet conditions are shown in Table 1.

4. Numerical implementations

The computational fluid dynamic codes are utilized by applying finite volume scheme and simple algorithm to solve the equations. Fig. 3 shows the algorithm (SIMPLE).

Grid independence tests were conducted to ensure that the solutions were independent of the grid size. The computational domains are divided into about 106,000 structured cells to minimize the numbers of iteration and maximize the accuracy. Nine hundred iteration were used for low current output and 1,100 for high current density, and the criterion convergence between accurate iterations is less than 10^{-7} for all variables. An IBM-PC-Pentium 5 (CPU speed is 2.4GHz) was used to solve the set of equations. The computational time for solving the set of equations was 6 h.

5. Results and discussions

For verification, the obtained data is compared with the experimental data of Al-Baghdadi et al. [38] for the straight channel (conventional PEMFCs) in

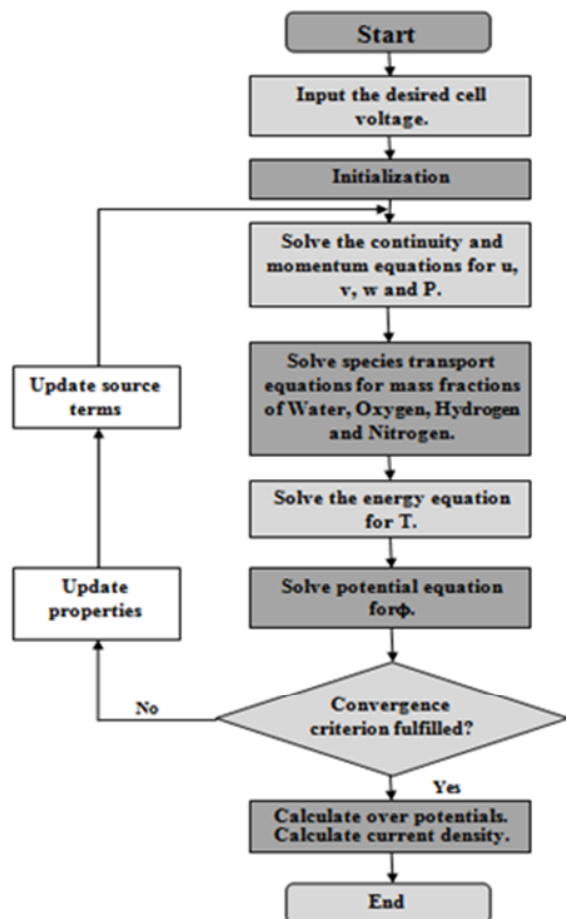


Fig. 3. The algorithm for numerical simulation in proton exchange membrane fuel cell.

Fig. 4. The comparison shows that the numerical model is in good agreement with the experimental data of Ref. [38] over a wide range of current density. However, a high rate of deviation is obvious between the numerical

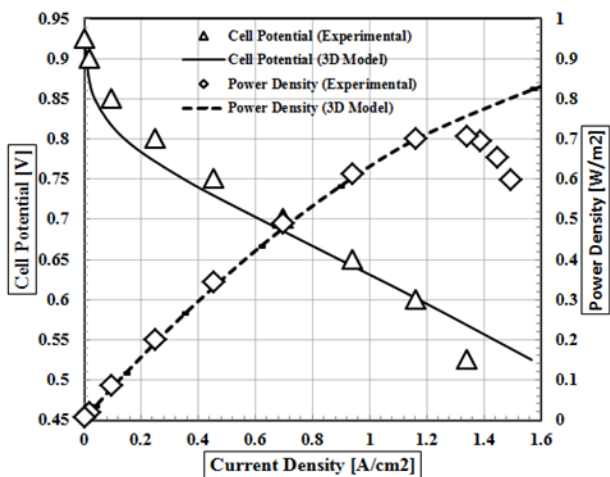


Fig. 4. Comparison of polarization curve of model with experimental data.

and experimental data at high current density. This is because the model ignores the liquid water by considering the water formed in the catalyst layer as the vapor phase in the numerical simulations. It should be noted that the liquid water fills the pores of the catalyst and gas diffusion layers and therefore prevents the oxygen molecules from reaching the catalyst surface. This phenomenon causes an uneven distribution of reactants; and consequently, a power loss which presents and compares by the experimental data in Fig. 4. The proposed concept, shown in Fig. 1, uses efficient channel geometry to improve conventional cell performance. This novel model leads to better distribution and access of the reactants at the GDL-channel interface under the same reactant flow rate and operation conditions. All the parametric and operating conditions used for the numerical simulations in this study are listed in Tables 1 and 2. These parameters have been taken from Ref. [37], which makes the model verification more accurate, see Ref. [38]. One of the most common ways to clarify the impact of the proposed architecture on cell performance is the comparison of the polarization curves of the new unconventional PEM fuel cell with the conventional cell. Fig. 5 shows a noticeable rate of increment in the polarization curve indicating that the novel configuration geometry produces more current density than the conventional straight channel. At PEMFCs typical operating condition of medium to high current density, the differences in current density values increase as the cell voltage

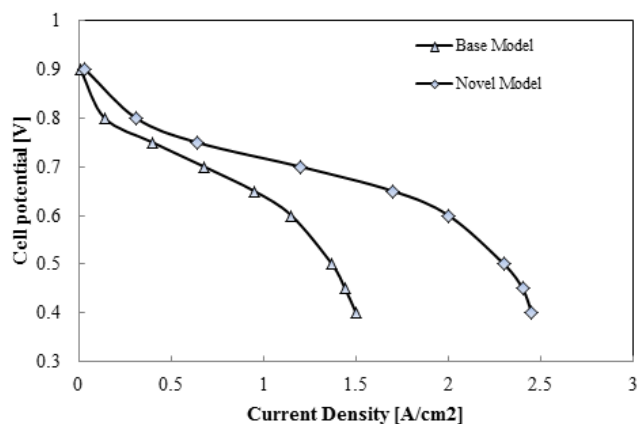


Fig. 5. The effect of novel geometry on the cell performance.

decreases, especially for the cell voltage of 0.4 V where the increments achieves an amazing value of about 50%. This implies that superior performance and higher current densities can be achieved by applying the introduced structure compared to the base model, and can be a good reason for considering as the base design in the next generation of PEMFCs stack.

To investigate the reason for the superior performance and the increment in outlet power, species distribution must be studied in the cell. Fig. 6 presents the hydrogen mass fraction at the anode side at a cell voltage of 0.4 V. As it is shown, the amount of hydrogen gradually decreases as it travels along the length of the channel. Although hydrogen is consumed from two side in each channel in the introduced configure, there is no dead zone, homogenous distribution is seen, and a high mass fraction region occupies the entire active area. Fig. 6 justifies the prior performance analysis. A high rate of reaction which causes substantial use of hydrogen in comparison with the base model is perceptible in the figure.

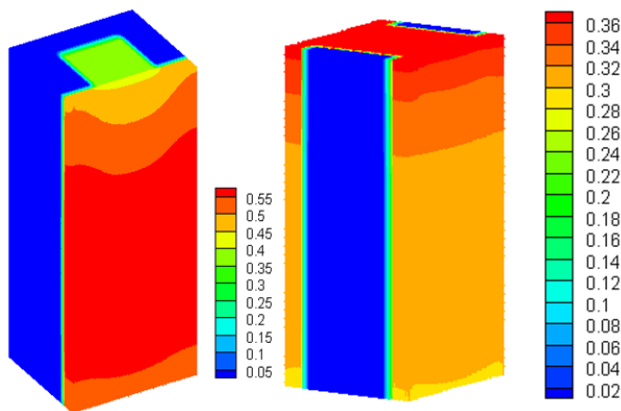


Fig. 6. Contours of Hydrogen mass fraction at the catalyst layer and gas diffusion layer of $V=0.4$.

The contour of oxygen distribution at the cathode catalyst, which is one of the main factors that affect the cell performance, is shown in Fig. 7 for $V = 0.4$ V. Fig. 6 demonstrates that the amount of oxygen decreases along the channel as it is consumed, and it is worth mentioning here that at low voltage. The higher current densities presented can be associated with the

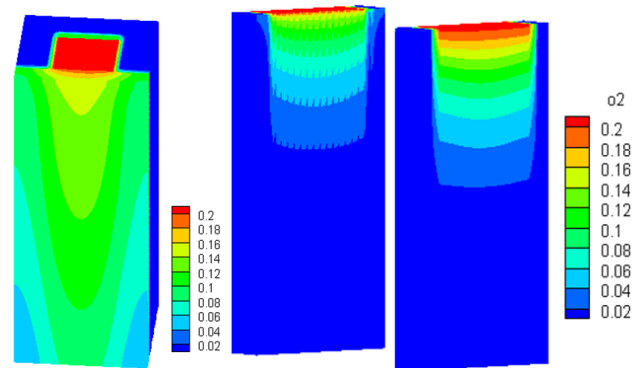


Fig. 7. Contours of oxygen mass fraction at the catalyst layer and gas diffusion layer at $V=0.4$ V.

high consumption of reactants and rate of chemical reaction at the CL-GDL interfaces.

It is well known that water management has an important role in the cell performance, especially on the membrane for proton transportation. Any variation in water may lead to the dehydration or flooding of the PEMFC, which should be controlled during the PEMFC operation. The water mass fraction distribution in the cell is presented in Fig. 8 for $V = 0.4$ V for the novel architecture.

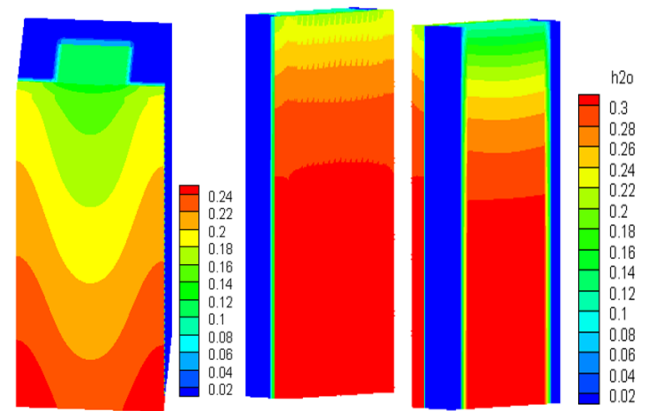


Fig. 8. Contours of water mass fraction at the catalyst layer and gas diffusion layer of cathode at $V=0.4$ V.

This figure clearly shows that the water generation and distribution are strongly dependent upon the flow field geometry. Fig. 8 also shows the water mass fraction increases along the channel. This is due to two reasons: the first reason is related to the water produced by oxygen consumption at the catalyst layer and the second can be attributed to the net water

transport from the anode side to the cathode side due to the electro-osmotic effects. It is observed from the contours that the water content increases along the channel due to chemical reactions generating a high value of water. An efficient concept must be able to deal with the water existing in the cell components, especially in the channel and GDL, which block the pores area at the reaction area and prevent the chemical reaction. One of the advantages of the novel geometries is its shorter channel length it can more efficiently remove the produced water, and promote the performance increment in high current density conditions.

Fig. 9 represents the temperature distribution at the cell voltage of 0.4 V in the mid cross section of the cell for the two configurations.

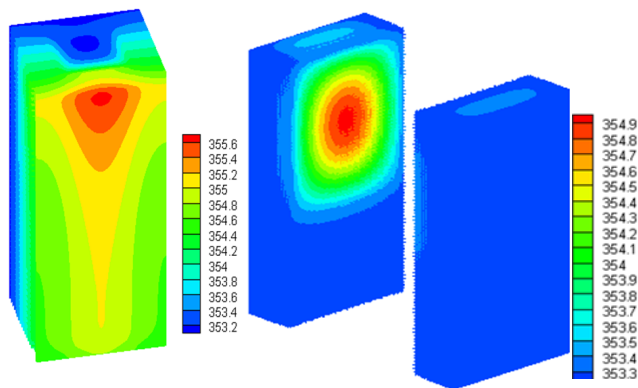


Fig. 9. Contours of Temperature at the catalyst layer and gas diffusion layer of cathode at $V=0.4$ V.

It can be observed that the maximum temperature inside the cell occurs at the cathode catalyst layer caused by the chemical reaction. Fig. 8 also shows a very low temperature region around the bipolar plates. This low temperature region in the shoulder zone is caused by the heat conduction through the adjacent bipolar plates. It should be noted that a small decrease in the temperatures of both cells is obvious along the channel as a result of water formation. The distribution of temperature reveals the trend of the minimum temperature occurring at the outlet region

of the novel geometry where more water is formed due to high rate of chemical reaction. Moreover, the temperature value of the novel flow field is within the temperature range of PEMFCs where the system will not experience mechanical stress due to a non-uniform distribution.

Current densities in the cells of the two configurations are depicted in Fig. 10 for the voltage of $V = 0.4$ V. The distribution of local current density illustrates a trend of high current density at the reactant inlet and low current density at the outlet. This trend can be associated to the reduction in the reactants concentration and the increasing water saturation at the GDL surface. Water increment causes limitations in the gas diffusion, resulting in concentration losses and a decreasing of current density. As shown in

Fig. 10, the increment of current density compared to the base model is calculated at about 50%, and the highest value is related to the GDLs-bipolar plates interfaces, which are the main gates for the output currents.

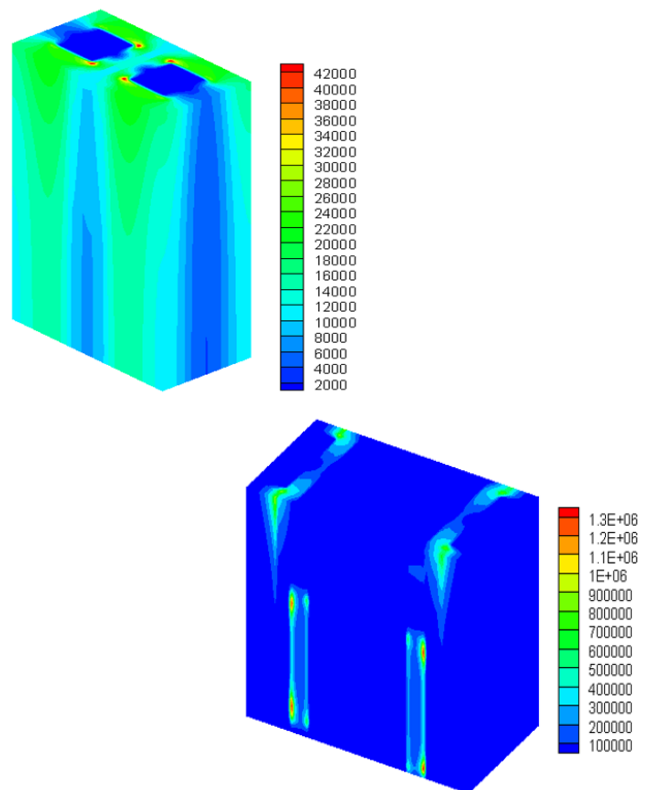


Fig. 10. Contours of current density distribution at the catalyst layer and gas diffusion layer of cathode at $V=0.4$ V.

6. Conclusion

A new PEM fuel cell flow channel was numerically simulated using a CFD program to address one of the critical economic challenges facing PEM fuel cells. The novel fuel cell flow channel was introduced to enhance performance by lowering the cost and size of the fuel cell stack. This new efficient flow field configuration accomplishes these goals: (i) good reactant spreading and diffusion over the electrode surface and a method of supplying gas to the flow field; (ii) the design of the flow field geometry for both anode and cathode; and (iii) decreasing cost and reducing size due to the dual connection and having two MEA in each channel. After analysis of the obtained data for the model, conventional geometry, and the polarization curve which is a good verification of channel geometry on the performance, it has been revealed the current densities values for the straight geometry with dual connection surpassed the current density region of the polarization curves of a fuel cell using the base structure by a large amount. Current density reached about 50% at the cell potential of 0.4 V increments in spite of having shorter lengths channels and up to 40% less occupied volume compared to the conventional (base) configuration of PEMFCs. Also, a higher rate of reaction due to high value of consumption, more uniform temperature, easy removal of produced water and high current density distribution can be achieved by the so-called geometry. In conclusion, this unique geometry with a dual connection in each channel demonstrated an improvement in terms of manufacturing fuel cell cost and performance operating at current densities due to the efficient use of channel geometry and better distribution and access of the reactants at the GDL-channel interface. Therefore, the presented structure can be considered as the base design for the next generation of PEMFCs stack.

Acknowledgment

The financial support of the Renewable Energy Organization of Iran is gratefully acknowledged (SUNA).

Nomenclature

a	Water activity
C	Molar concentration (mol/m ³)
D	Mass diffusion coefficient (m ² /s)
F	Faraday constant (C/mol)
I	Local current density (A/m ²)
J	Exchange current density (A/m ²)
K	Permeability (m ²)
M	Molecular weight (kg/mol)
nd	Electro-osmotic drag coefficient
P	Pressure (Pa)
R	Universal gas constant (J/mol-K)
T	Temperature (K)
t	Thickness
V	Cell voltage
V _{oc}	Open-circuit voltage
W	Width
X	Mole fraction

Greek Letters:

α	Water transfer coefficient
ϵ_{eff}	Effective porosity
ρ	Density (kg/m ³)
μ	Viscosity (kg/m-s)
σ_e	Membrane conductivity (1/ohm-m)
λ	Water content in the membrane
ζ	Stoichiometric ratio
η	Over potential (v)
λ_{eff}	Effective thermal conductivity (w/m-k)

Subscripts and Superscripts:

a	Anode
c	Cathode
cl	Catalyst
GDI	Gas diffusion layer
ch	Channel
k	Chemical species
m	Membrane
MEA	Membrane electrolyte assembly
ref	Reference value
sat	saturated
w	Water

7. References

- [1] Kim YS., Kim SI., Lee NW., Kim MS., Study on a purge method using pressure reduction for effective water removal in polymer electrolyte membrane fuel cells”, *Int. J. Hydrogen Energy*, 2015, 40: 9473.
- [2] Taspinara R., Litster S., Kumbur EC., “A computational study to investigate the effects of the bipolar plate and gas diffusion layer interface in polymer electrolyte fuel cells”, *Int. J. Hydrogen Energy*, 2015, 40: 7124.
- [3] Verma A., Pitchumani R., “Influence of transient operating parameters on the mechanical behavior of fuel cells”. *Int. J. Hydrogen Energy*, 2015, 40: 8442.
- [4] Jeon Y., Na H., Hwang H., Park J., Hwang H., Shul Y., “Accelerated life-time test protocols for polymer electrolyte membrane fuel cells operated at high temperature. *Int. J. Hydrogen Energy*, 2015, 40: 3057.
- [5] Sadeghifar H., Djilali N., Bahrami M., “ Effect of polytetrafluoroethylene (PTFE) and micro porous layer (MPL) on thermal conductivity of fuel cell gas diffusion layers: modeling and experiments. *J. Power Sources*, 2014, 248: 632.
- [6] Sadeghifar H., Bahrami M., Djilali N., A statistically based thermal conductivity model for PEMFC gas diffusion layers. *J. Power Sources*, 2013, 233: 369.
- [7] Sadeghifar H., Djilali N., Bahrami M., “A new model for thermal contact resistance between fuel cell gas diffusion layers and bipolar plates”, *J. Power Sources*, 2014, 266: 51.
- [8] Sadeghifar H., Djilali N., Bahrami M., “Thermal conductivity of a graphite bipolar plate (BPP) and its thermal contact resistance with fuel cell gas diffusion layers: effect of compression, PTFE, micro porous layer (MPL), BPP out-of-flatness and cyclic load”, *J. Power Sources*, 2015, 273: 96.
- [9] Mert SO., Ozcelik Z., Dincer I. “ Comparative assessment and optimization of fuel cells”, *Int. J. Hydrogen Energy*, 2015, 40: 7835.
- [10] Wei Zh., Su K., Sui Sh., He A, Du Sh. “High performance polymer electrolyte membrane fuel cells (PEMFCs) with gradient Pt nanowire cathodes prepared by decal transfer method”, *Int. J. Hydrogen Energy*, 2015, 40: 3068.
- [11] Limjeeararus N., Charoen-amornkitt P., “ Effect of different flow field designs and number of channels on performance of a small PEFC”, *Int. J. Hydrogen Energy*, 2015, 40: 7144.
- [12] Arvay A, French J, Wang JC, Peng XH, Kannan AM. “ Nature inspired flow field designs for proton exchange membrane fuel cell”, *Int. J. Hydrogen Energy*, 2013, 38: 3717.
- [13] Hsieh SS., Yang SH., Kuo JK., Huang CF., Tsai HH., “ Study of operational parameters on the performance of micro PEMFCs with different flow fields”, *Energy Convers Manage*, 2006, 47: 1868.
- [14] Torkavannejad A., pesteei M., Khalilian M., Ramin F., Mirzaee I., “ Effect of Deflected Membrane Electrode Assembly on Species Distribution in PEMFC”. *Int. J. Eng., transactions c*: 2015, 28: 893.
- [15] Yuh MF., Su A., “A three-dimensional full-cell CFD model used to investigate the effects of different flow channel designs on PEMFC performance”. *Int. J. Hydrogen Energy*, 2007, 32: 4466.
- [16] Lorenzini-Gutierrez D., Hernandez-Guerrero A., Ramos-Alvarado B., Perez-Raya I., Alatorre-Ordaz A., “ Performance analysis of a proton exchange membrane fuel cell using tree-shaped designs for flow distribution”, *Int. J. Hydrogen Energy*, 2013, 38: 14750.
- [17] Sierra J., Figueroa-Ramírez S.J., Díaz S.E., Vargas J, Sebastian P.J., “ Numerical evaluation of PEM fuel cell with conventional flow fields adapted to tubular plates”, 2014, 39: 16694.

- [18] Pourmahmoud N., Rezazadeh S, Mirzaee I., Motaleb Faed S., " A computational study of a three-dimensional proton exchange membrane fuel cell (PEMFC) with conventional and deflected membrane electrode". *J. Mech. Sci. Technol.*, 2012, 26: 2959.
- [19] Escobar-Vargas J.A., Hernandez-Guerrero A., Alatorre Ordaz A., Damian-Ascencio C.E., Elizalde-Blancas F., "Performance of a non-conventional flow field in a PEMFC". Paper presented at the 20th International Conference on Efficiency, Cost, Optimization Simulation and Environmental Impact of Energy Systems, Padova, Italy, 2007, 23:534.
- [20] Juarez-Robles D., Hernandez-Guerrero A., Ramos-Alvarado B., Elizalde-Blancas F., Damian-Ascencio CE., " Multiple concentric spirals for the flow field of a proton exchange membrane fuel cell". *J. Power Sources* 2011, 196: 8019.
- [21] Cano-Andrade S., Hernandez-Guerrero A., Von-Spakovsky MR., Rubio-Arana C., "Effect of the radial plate flow field distribution on current density in a proton exchange membrane (PEM) fuel cell". Paper presented at the ASME International Mechanical Engineering Congress and Exposition, Seattle-Washington, United States of America, 2007, 11.
- [22] Cano-Andrade S., Hernandez-Guerrero A., Von Spakovsky MR., Damian-Ascencio CE., Rubio-Arana JC., " Current density and polarization curves for radial flow field patterns applied to PEMFCs (proton exchange membrane fuel cells)". *Energy*, 2010, 35: 920.
- [23] Torkavannejad A, Sadeghifar H, Pourmahmoud N, Ramin F. Novel architectures of polymer electrolyte membrane fuel cells: Efficiency enhancement and cost reduction. *Int. J. Hydrogen Energy*, 2015, 40: 12466.
- [24] Wang X.D., Huang Y.X, Cheng C.H., Jang J.Y., Lee D.J, Yan W.M., et al. "An inverse geometry design problem for optimization of single serpentine flow field of PEM fuel cell". *Int. J. Hydrogen Energy*, 2010, 35:4247.
- [25] Ramos-Alvarado B., Hernandez-Guerrero A., Juarez-Robles D., Li L., " Numerical investigation of the performance of symmetric flow distributors as flow channels for PEM fuel cells international". *Int. J. Hydrogen Energy* 2012, 37: 436.
- [26] Chen Y.S., Peng H., " Predicting current density distribution of proton exchange membrane fuel cells with different flow field designs". *J. Power Sources* 2011, 196: 1992.
- [27] Cano-Andrade S., Hernandez-Guerrero A., von Spakovsky MR., Damian-Ascencio C.E., Rubio-Arana JC., Current density and polarization curves for radial flow field patterns applied to PEMFCs. *Energy*, 2010, 35: 920.
- [28] Friess BR., Hoorfar M., "Development of a novel radial cathode flow field for PEMFC". *Int. J. Hydrogen Energy* 2012, 37: 7719.
- [29] Surajudeen Olanrewaju O., "Performance enhancement in proton exchange membrane fuel cell-numerical modeling and optimization [PhD thesis]". University of Pretoria, 2012.
- [30] Juarez-Robles., D., Hernandez-Guerrero., A., Damian-Ascencio., C. E., Rubio-Arana, C., "Three dimensional analysis of a PEM fuel cell with the shape of a fermat spiral for the flow channel configuration", *Proceedings of IMECE2008, ASME International Mechanical Engineering Congress and Exposition* October, Boston, Massachusetts, USA, 2008, 8:5421.
- [31] Friess BR., "Development of radial flow channel for improved water and gas management of cathode flow field in polymer electrolyte membrane fuel cell"[Masters of Applied Science Thesis]. University of British Columbia; 2010.
- [32] Soong CY., Yan WM., Tseng CY., Liu HC., Chen F., Chu HS., " Analysis of reactant gas transport in a PEM fuel cell with partially blocked fuel flow channels". *J. Power Sources*, 2005, 143: 36.
- [33] Walczyk D.F., Sangra J.S., "A feasibility study of

Ribbon architecture for PEM fuel cells'. ASME, J. Fuel Cell Sci. Technol. 2010, 7: 5101.

[34] Tseng C., Tsang Tsai B., Liu Zh., Cheng T., Chang W, Lo Sh., " A PEM fuel cell with metal foam as flow distributor", Energy Conversion and Management, 2012, 62: 14.

[35] Bilgili M, Bosomoiu M , Tsotridis G, Gas flow field with obstacles for PEM fuel cells at different operating conditions, Int. J. Hydrogen Energy. 2013, 40: 2303.

[36] Vazifeshenas Y., Sedighi k., Shakeri M., "Numerical investigation of a novel compound flow field for PEMFC performance improvement", Int. J. Hydrogen Energy 2015, 40: 15032.

[37] Khazae I., Ghazikhani M., "Three-dimensional modeling and development of the new geometry PEM fuel cell". Arabian J. Sci. Eng., 2013, 38: 1551.

[38] Sadiq Al-Baghdadi Maher A.R., Shahad Al-Janabi Haroun A.K., "Parametric and optimization study of a PEM fuel cell performance using three-dimensional computational fluid dynamics model". Renew Energy, 2007, 32: 1077.